frontiers in Chemistry

ORIGINAL RESEARCH
published: 24 July 2018
doi: 10.3389/fchem.2018.00283

Effect of Environmental Temperature on the Content of Impurity $Li_3V_2(PO_4)_3$/C in $LiVPO_4F$/C Cathode for Lithium-ion Batteries

Taotao Zeng[1], *Changling Fan*[1,2]*, *Zheng Wen*[1], *Qiyuan Li*[1], *Zeyan Zhou*[1], *Shaochang Han*[1] *and Jinshui Liu*[1,2]*

[1] College of Materials Science and Engineering, Hunan University, Changsha, China, [2] Hunan Province Key Laboratory for Advanced Carbon Materials and Application Technology, Hunan University, Changsha, China

Previous studies have shown that the impurity $Li_3V_2(PO_4)_3$ in $LiVPO_4F$ will adversely affect its electrochemical performance. In this work, we show that the crystalline composition of $LiVPO_4F$/C is mainly influenced by the environmental temperature. The content of $Li_3V_2(PO_4)_3$ formed in $LiVPO_4F$/C is 0, 11.84 and 18.75% at environmental temperatures of 10, 20, and 30°C, respectively. For the sample LVPF-30C, the SEM pattern shows a kind of alveolate microstructure and the result of selected area electron diffraction shows two sets of patterns. The $LiVPO_4F$/C cathode without impurity phase $Li_3V_2(PO_4)_3$ was prepared at 10°C. The selected area electron diffraction result proves that the lattice pattern of $LiVPO_4F$ is a regular parallelogram. Electrochemical tests show that only one flat plateau around 4.2 V appears in the charge/discharge curve, and the reversible capacity is 140.4 mAh·g^{-1} at 0.1 C, and 116.3 mAh·g^{-1} at 5 C. From these analyses, it is reasonable to speculate that synthesizing $LiVPO_4F$/C at a low environmental temperature is a practical strategy to obtain pure crystalline phase and good electrochemical performance.

Keywords: lithium-ion batteries, lithium vanadium fluorophosphates, environmental temperature, alveolate structure, electrochemical performance

OPEN ACCESS

Edited by:
Jiexi Wang,
Central South University, China

Reviewed by:
Xianwen Wu,
Jishou University, China
Jie Shu,
Ningbo University, China
Guochun Yan,
Collège de France, France
Haoran Jiang,
Hong Kong University of Science and Technology, Hong Kong

***Correspondence:**
Changling Fan
fancl@hnu.edu.cn
Jinshui Liu
jsliu@hnu.edu.cn

Specialty section:
This article was submitted to Physical Chemistry and Chemical Physics, a section of the journal Frontiers in Chemistry

Received: *26 April 2018*
Accepted: *22 June 2018*
Published: *24 July 2018*

Citation:
Zeng T, Fan C, Wen Z, Li Q, Zhou Z, Han S and Liu J (2018) Effect of Environmental Temperature on the Content of Impurity $Li_3V_2(PO_4)_3$/C in $LiVPO_4F$/C Cathode for Lithium-ion Batteries. Front. Chem. 6:283. doi: 10.3389/fchem.2018.00283

INTRODUCTION

The rechargeable lithium-ion battery has been widely studied because of its applications in electric vehicles, mobile phones, and energy storage devices (Huang et al., 2009; Konarov et al., 2017). $LiFePO_4$ delivers superior thermal stability and excellent cyclic performance, but a low working potential decreases its energy density (Yamada et al., 2003; Kim et al., 2015; Eftekhari, 2017; Wu et al., 2017).

A novel cathode lithium vanadium fluorophosphate ($LiVPO_4F$) material has been reported (Gover et al., 2006). The working potential (4.2 V) of $LiVPO_4F$ is much higher than that of $LiFePO_4$ and $LiCoO_2$ (Ma et al., 2013a; Hu et al., 2014; Wu et al., 2016). Moreover, the thermal stability of $LiVPO_4F$ is better than that of $LiFePO_4$ and $LiCoO_2$ (Wang et al., 2014; Xu et al., 2015). If the shortcoming of electronic conductivity is solved, $LiVPO_4F$ will be an outstanding cathode material (Reddy et al., 2010; Ma et al., 2013b; Satish et al., 2016). Some improvements have been adjusted to $LiVPO_4F$ cathode, such as cation doped, carbon coated and various synthesized routes (Wang et al., 2013a; Liu et al., 2016; Wu et al., 2018). Recently, adopting

facile and controllable methods to prepare $LiVPO_4F$ is the key areas of research. $LiVPO_4F$ was reported by two-step carbothermal reduction in some references. However, this method suffers from high energy consumption and a large content of carbon, because the intermediate VPO_4 is prepared separately at 700–800°C (Ma et al., 2014; Liu et al., 2015; Wang et al., 2016).

Thus, a novel one-step method in which the synthesis of VPO_4 is omitted and carbon content is restricted to a very low level is of great research interest. Although the electrochemical performance of $LiVPO_4F$ prepared is improved, the plateaus belonging to impurity $Li_3V_2(PO_4)_3$ come into being (Liu et al., 2012; Wang et al., 2013b; Xiao et al., 2013). Therefore, the formation of $Li_3V_2(PO_4)_3$ is observed even though we use a synthesis method that employs a novel chemical reduction route. The content of $Li_3V_2(PO_4)_3$ should be carefully controlled because it may adversely affect the performance of the $LiVPO_4F$ cathode.

In this work, we discovered that the formation of impurity $Li_3V_2(PO_4)_3$ is directly related to the environmental temperature. The formation mechanism was investigated through further analysis of the structure and synthesis procedures.

EXPERIMENTAL

Materials Synthesis

$LiVPO_4F$/C was synthesized by using a novel chemical reduction method. The chemical reagent used was of analytical reagent grade. 0.03 mol $H_2C_2O_4$ dissolved in deionized water was used as a chelating agent and reducing agent. 0.01 mol V_2O_5 was added slowly under vigorous magnetic stirring at 60°C. LiF and $NH_4H_2PO_4$ at the molar ratio of 1:1 to vanadium were introduced in after 10 min. A PVDF carbon source of 1.4943 g was dispersed in 30 ml water in a solution of hexadecyl trimethyl ammonium bromide under ultrasonic assistance at 50°C. Subsequently, the PVDF suspension was added to the reaction system. Finally, the suspension was dried overnight in vacuum at 85°C. The precursor was presintered at 400°C for 5 h and sintered at 800°C for 4 h in a tubular furnace with flowing high-purity argon.

Characterization

The crystal structure of the material was examined by X-ray diffraction (XRD, Rigaku D/MAX 2500). The morphology and elemental content were investigated with scanning electron microscopy (SEM, Navo NanoSEM230) and energy disperse spectroscopy (EDS). Nanoscale morphology and selected area electron diffraction (SAED) were performed by using high-resolution transmission electron microscopy (HRTEM, JEOL-3010).

Electrochemical Test

The electrochemical performance of $LiVPO_4F$/C electrodes was evaluated using an Arbin BT2000 battery test system. The cathode film was fabricated by mixing $LiVPO_4F$/C (80 wt.%), acetylene black (15 wt.%), and PVDF (5 wt.%) in the solvent N-methyl pyrrolidone, and the slurry was coated on an aluminum collector. The electrodes were dried in a vacuum oven at 120°C for 12 h and 2016 coin-type cells were assembled in a glove box (S1220/750). The electrolyte was 1.3 $mol{\cdot}L^{-1}$ $LiPF_6$ in a mixing solvent of ethylene carbonate, dimethyl carbonate, and ethyl methyl carbonate (1:1:1). A lithium foil and a polypropylene separator (Celgard 2400) were used as counter electrode and separator, respectively.

RESULTS AND DISCUSSION

The electrochemical performance of triclinic $LiVPO_4F$/C is partially determined by the content of impurity $Li_3V_2(PO_4)_3$/C in it. Our study revealed that $LiVPO_4F$ prepared at a high environmental temperature delivers poor performance. To investigate the reason for this, we synthesized $LiVPO_4F$/C at different environmental temperatures (30, 20, and 10°C), and named the respective samples as LVPF-30C, LVPF-20C, and LVPF-10C.

The XRD patterns of the samples are shown in **Figure 1A**. The main diffraction peaks correspond to a triclinic system with the space group of P-1, and can be indexed as the standard pattern of $LiVPO_4F$ (Barker et al., 2003; Huang et al., 2009). The absence of peaks corresponding to crystalline carbon proves that carbon is amorphous. No impurity peaks in LVPF-10C, which delivers the strongest peaks among the samples, was found. The refined cell parameters a, b, and c were 5.174, 5.308, and 7.509 Å, and the cell volume was 174.18 $Å^3$. These results compare well with the classic results reported by Barker (Barker et al., 2005). However, the peaks at 20.69°, 23.53°, and 24.48° belonging to the impurity $Li_3V_2(PO_4)_3$ (symbol # in **Figure 1A**) occur in the curves of LVPF-30C and LVPF-20C (Zhu et al., 2008). The percentages of $Li_3V_2(PO_4)_3$ in $LiVPO_4F$ were estimated by refining the XRD patterns in **Figure 1B**. The content of $Li_3V_2(PO_4)_3$ increased gradually from 0% (10°C) to 11.84% (20°C) and 18.75% (30°C). Hence, our preliminary presumption is that low environmental temperature plays an important role in the preparation of pure $LiVPO_4F$.

In **Figure 1C**, four flat plateaus (A, B, C, and D) appear in the discharge curves of LVPF-30C. The predominant plateau A around 4.2 V is attributed to $LiVPO_4F$/C, and is in accordance with Barker's work (Barker et al., 2003), and B, C, and D are assigned to $Li_3V_2(PO_4)_3$/C. The specific capacities at 0.1 C and 5 C are 138.6 and 101.1 $mAh{\cdot}g^{-1}$. However, when temperature drops to 20°C (corresponding to LVPF-20C, **Figure 1D**), the plateaus of $Li_3V_2(PO_4)_3$/C are shorter than before, establishing the decreasing content of impurity. The specific capacity increases obviously, especially at 5 C (118.3 $mAh{\cdot}g^{-1}$). Further, only a plateau A at 4.2 V without other plateaus of impurity $Li_3V_2(PO_4)_3$/C is observed in LVPF-10C (**Figure 1E**). It is important to note that $Li_3V_2(PO_4)_3$/C disappear entirely. The specific capacities at 0.1 C 1 C and 5 C are 140.4 $mAh{\cdot}g^{-1}$, 130.6 $mAh{\cdot}g^{-1}$ and 116.3 $mAh{\cdot}g^{-1}$, which are very close to that of LVPF-20C in **Figure 1F**. LVPF-30C delivers the worst performance at a high current density. LVPF-20C with 11.84%

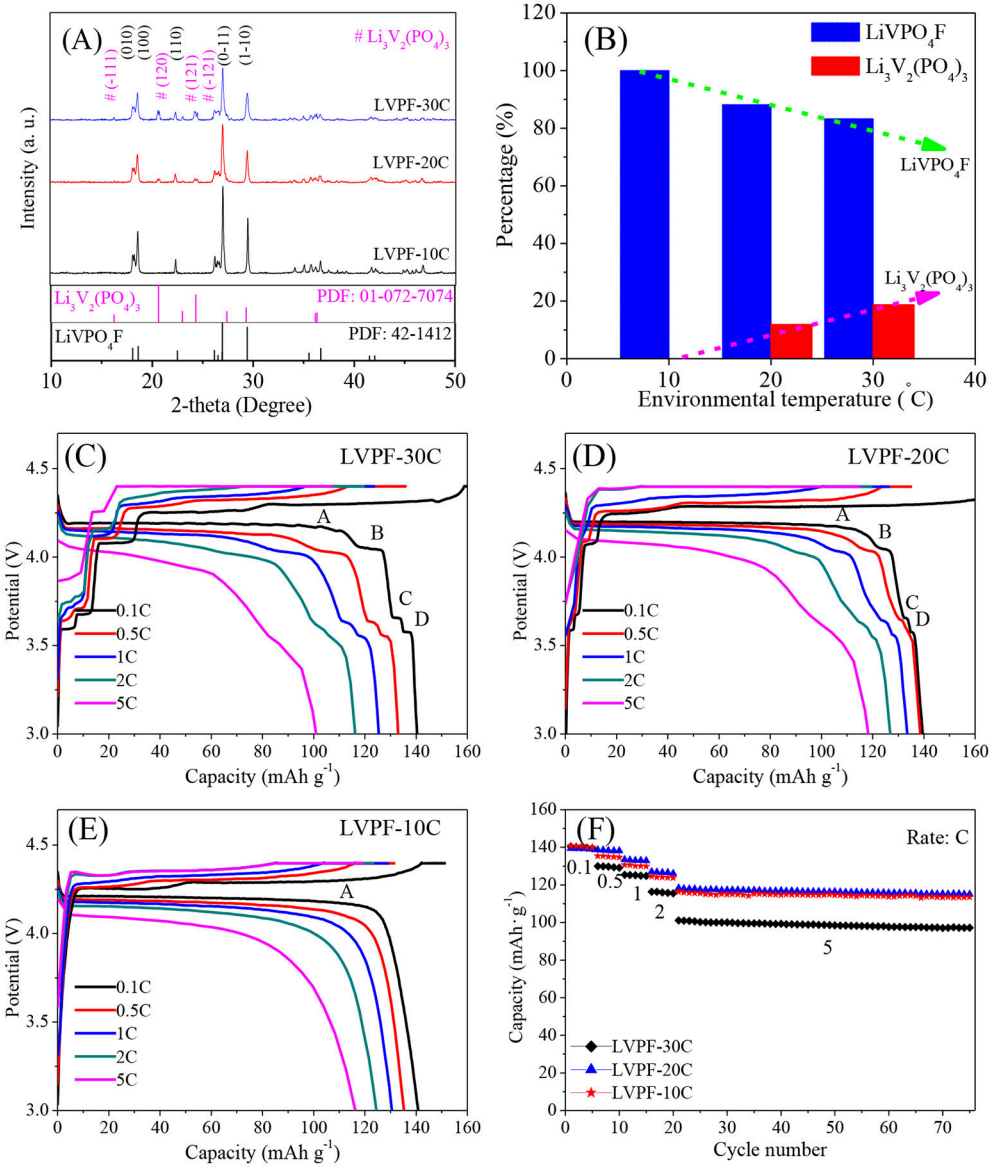

FIGURE 1 | XRD patterns of $LiVPO_4F$/C **(A)**, percentage of $Li_3V_2(PO_4)_3$ in $LiVPO_4F$/C **(B)**, and charge/discharge curves of $LiVPO_4F$/C **(C–F)**.

impurity $Li_3V_2(PO_4)_3$/C possesses the optimum capacity at a high current density. The reason is that $Li_3V_2(PO_4)_3$/C is a fast ion conductor and allows a fast transfer of lithium ions in the cathode. Nevertheless, an excess of the impurity $Li_3V_2(PO_4)_3$/C in $LiVPO_4F$/C adversely affects the rate and the cycling capability.

In **Figure 2A**, the alveolate structure can be easily observed in LVPF-30C. The surface of most particles is broken. This structure is observed in the HRTEM image. The SAED pattern is made up of two sets of lattices with different characteristics (inset of **Figure 2B**). These parallelogram lattices are attributed to triclinic $LiVPO_4F$ (bottom) and monoclinic $Li_3V_2(PO_4)_3$ (top). In **Figure 2C**, the EDS image in the alveolate field proves the existence of $Li_3V_2(PO_4)_3$ distinctly because the content of fluorine is much lower than that of vanadium. **Figures 2D,E** show that vanadium is uniformly distributed on the surface of particles and a small quantity of fluorine is detected. This proves that impurity $Li_3V_2(PO_4)_3$ without fluorine is formed in the alveolate zone.

There is no alveolate structure on the flawless surface of LVPF-10C (**Figure 2F**) and the lattice fringes can be clearly observed (**Figure 2G**). The pattern of SAED in the square frame is a typical parallelogram, and is similar to the bottom lattice in **Figure 2B**. This pattern is attributed to the typical crystalline form of $LiVPO_4F$ with the triclinic system. Thus, LVPF-10C possesses a good crystalline morphology with a thin layer covering on the surface of the crystalline $LiVPO_4F$. Its lattice pattern is a series

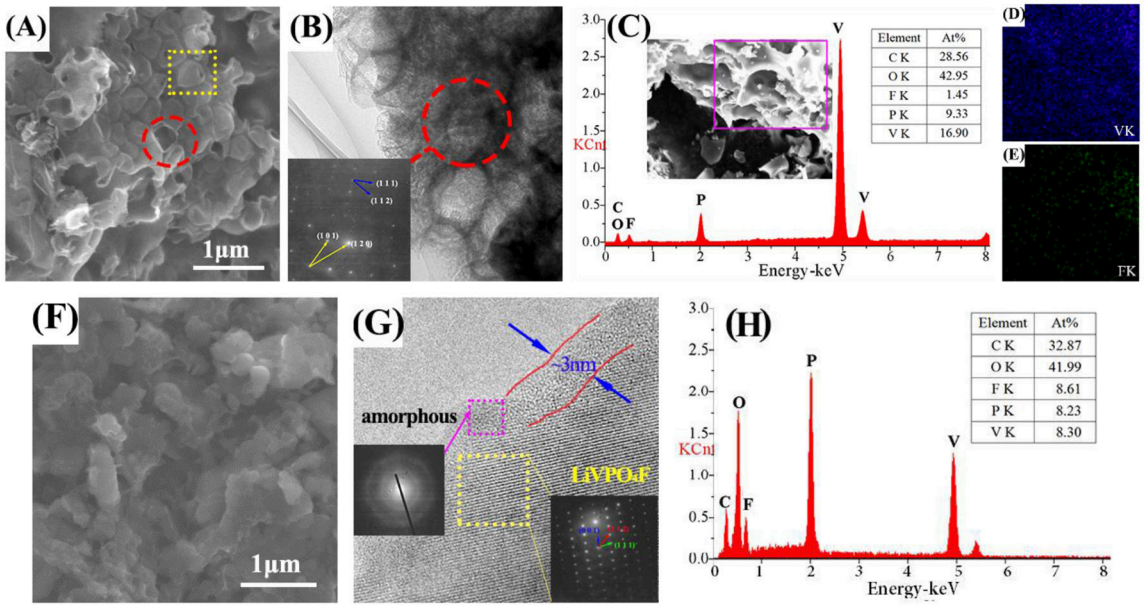

FIGURE 2 | SEM, HRTEM, SAED, and EDS images of LVPF-30C **(A–E)** and LVPF-10C **(F–H)**.

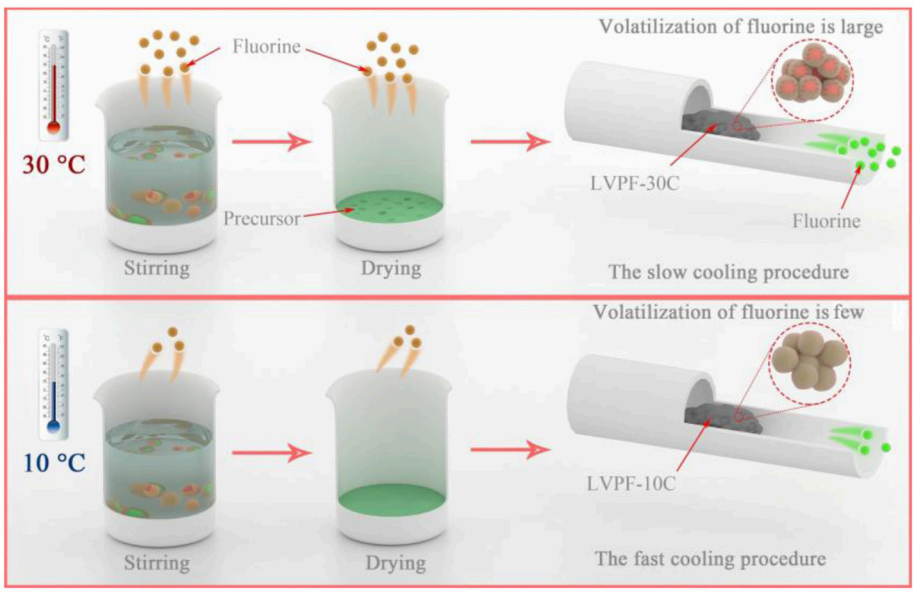

FIGURE 3 | Schematic of the volatilization of fluorine at environmental temperatures of 30°C and 10°C.

of concentric circles, which is the characteristic of amorphous carbon (Song et al., 2008). The atomic contents of vanadium and fluorine are 8.61 and 8.30%, respectively, and match well with the atomic ratio of $LiVPO_4F$ in **Figure 2H**. Thus, we conclude that low temperature (10°C) helps to prepare pure phase $LiVPO_4F$.

The formation mechanism of the alveolate structure is investigated in **Figure 3**. On one hand, the excessive oxalic acid hydrolyzes in deionized water and produces hydrogen ions in aqueous solution. Ammonium dihydrogen phosphate generates ammonium ions in the hydrolysis reaction. A fluoride compound is formed when a hydrogen ion and an ammonium ion are combined with a fluoride ion released by LiF. Therefore, HF and NH_4F are formed in the reaction (Zhou et al., 2009). It is well known that fluoride compounds are unstable and easily evaporate. From the viewpoint of reaction kinetics, the volatilization rate of fluoride will increase at least 6 to 8 times

at 30°C compared to 10°C in reaction and drying. Therefore, the content of fluorine in the precursor at 30°C is evidently lower than that at 10°C. It can be inferred that the impurity $Li_3V_2(PO_4)_3$ is formed in this condition. On the other hand, the temperature of the tubular furnace drops slowly at 30°C. The cooling rate of LVPF-30C is lower than that of LVPF-10C. The longer cooling time of LVPF-30C accelerates the evaporation of fluoride, especially at 600–800°C. Therefore, this ensures that the fluorine content in LVPF-30C is much less than the value determined. The impurity $Li_3V_2(PO_4)_3$ is formed, which is in accordance with the above analysis of its structure and morphology.

Hence, the volatilization of fluoride should be inhibited in the preparation processes of $LiVPO_4F$. Based on all of the evidence we have presented above, we legitimately conclude that a lower environmental temperature is more helpful to synthesize a $LiVPO_4F$/C cathode with a low content of impurity and excellent electrochemical performance.

CONCLUSIONS

A sample of LVPF-10C, which was prepared at an environmental temperature of 10°C, exhibited a regular parallelogram space pattern that is attributed to the pure triclinic form of $LiVPO_4F$. High environmental temperature accelerates the volatilization of fluoride in the drying and sintering process and decreases the fluorine content. Then, a large quantity of $Li_3V_2(PO_4)_3$ reduces the plateaus in the discharge curves and deteriorates the rate of performance in LVPF-30C. Therefore, our work is devoted to give a direction to improve the synthetic process and advise what we need to do in the future.

AUTHOR CONTRIBUTIONS

TZ wrote the paper and designed the main part of the experiment. CF was the main advisor. ZW and QL carried out material preparation and the electrochemical test. ZZ discussed and refined the paper. TZ, CF, ZW, QL, and ZZ proposed the research. CF, SH, and JL obtained the main financial support for the research and supervised all the experiments.

ACKNOWLEDGMENTS

This work was supported by the National Natural Science Foundation of China [51472082, 51672079, 51372079] and science and technology project of Changsha City [k1508010–11].

REFERENCES

Barker, J., Gover, R. K. B., Burns, P., Bryan, A., Saidi, M. Y., and Swoyer, J. L. (2005). Structural and electrochemical properties of lithium vanadium fluorophosphate, $LiVPO_4F$. *J. Power Sources* 146, 516–520. doi: 10.1016/j.jpowsour.2005.03.126

Barker, J., Saidi, M. Y., and Swoyer, J. L. (2003). Electrochemical insertion properties of the novel lithium vanadium fluorophosphate, $LiVPO_4F$. *J. Electrochem. Soc.* 150, A1394–A1398. doi: 10.1016/j.ssi.2003.09.009

Eftekhari, A. (2017). $LiFePO_4$/C nanocomposites for lithium-ion batteries. *J. Power Sources* 343, 395–411. doi: 10.1016/j.jpowsour.2017.01.080

Gover, R. K. B., Burns, P., Bryan, A., Saidi, M. Y., Swoyer, J. L., and Barker, J. (2006). $LiVPO_4F$: a new active material for safe lithium-ion batteries. *Solid State Ionics* 177, 2635–2638. doi: 10.1016/j.ssi.2006.04.049

Hu, G. R., Cao, J. C., Peng, Z. D., Cao, Y. B., and Du, K. (2014). Enhanced high-voltage properties of $LiCoO_2$ coated with $Li[Li_{0.2}Mn_{0.6}Ni_{0.2}]O_2$. *Electrochim. Acta* 149, 49–55. doi: 10.1016/j.electacta.2014.10.072

Huang, H., Faulkner, T., Barker, J., and Saidi, M. Y. (2009). Lithium metal phosphates, power and automotive applications. *J. Power Sources* 189, 748–751. doi: 10.1016/j.jpowsour.2008.08.024

Kim, M., Lee, S., and Kang, B. (2015). Fast-rate capable electrode material with higher energy density than $LiFePO_4$:4.2V $LiVPO_4F$ synthesized by scalable single-Step solid-state reaction. *Adv. Sci. (Weinh)* 3:1500366. doi: 10.1002/advs.201500366

Konarov, A., Myung, S. T., and Sun, Y. K. (2017). Cathode materials for future electric vehicles and energy storage systems. *Acs Energy Lett.* 2, 703–708. doi: 10.1021/acsenergylett.7b00130

Liu, J. Q., Zhong, S. K., Ling, W. U., Kang, W., and Fan, L. Ü. (2012). Electrochemical performance of $LiVPO_4F$/C synthesized by different methods. *Chin. J. Power Sources* 22, s157–s161. doi: 10.1016/S1003-6326(12)61702-6

Liu, Z., Peng, W., Fan, Y., Li, X., Wang, Z., Guo, H., et al. (2015). One-step facile synthesis of graphene-decorated $LiVPO_4F$/C nanocomposite as cathode for high-performance lithium ion battery. *Ceram. Int.* 41, 9188–9192. doi: 10.1016/j.ceramint.2015.03.090

Liu, Z., Peng, W., Shih, K., Wang, J., Wang, Z., Guo, H., et al. (2016). A MoS_2 coating strategy to improve the comprehensive electrochemical performance of $LiVPO_4F$. *J. Power Sources* 315, 294–301. doi: 10.1016/j.jpowsour.2016.02.083

Ma, R., Shao, L., Wu, K., Shui, M., Ren, Y., and Shu, J. (2013a). Comparison of $LiVPO_4F$ to $Li_4Ti_5O_{12}$ as anode materials for lithium-ion batteries. *ACS Appl. Mater. Inter.* 5, 8615–8627. doi: 10.1021/am402132u

Ma, R., Shao, L., Wu, K., Shui, M., Wang, D., and Shu, J. (2014). Effects of oxidation on structure and performance of $LiVPO_4F$ as cathode material for lithium-ion batteries. *J. Power Sources* 248, 874–885. doi: 10.1016/j.jpowsour.2013.10.029

Ma, R., Shu, J., Lu, H., Miao, S., Shao, L., Wang, D., et al. (2013b). Ex situ FTIR spectroscopy study of $LiVPO_4F$ as cathode material for lithium-ion batteries. *Ionics (Kiel).* 19, 725–730. doi: 10.1007/s11581-012-0807-8

Reddy, M. V., Rao, G. V. S., and Chowdari, B. V. R. (2010). Long-term cycling studies on 4 V-cathode, lithium vanadium fluorophosphate. *J. Power Sources* 195, 5768–5774. doi: 10.1016/j.jpowsour.2010.03.032

Satish, R., Aravindan, V., Ling, W. C., and Madhavi, S. (2016). $LiVPO_4F$: a new cathode for high-energy lithium ion capacitors. *Chemistryselect* 1, 3316–3322. doi: 10.1002/slct.201600912

Song, M. S., Kim, D. Y., Kang, Y. M., Kim, Y. I., Lee, J. Y., and Kwon, H. S. (2008). Amphoteric effects of Fe_2P on electrochemical performance of lithium iron phosphate-carbon composite synthesized by ball-milling and microwave heating. *J. Power Sources* 180, 546–552. doi: 10.1016/j.jpowsour.2008.01.079

Wang, J., Liu, Z., Yan, G., Li, H., Peng, W., Li, X., et al. (2016). Improving the electrochemical performance of lithium vanadium fluorophosphate cathode material: focus on interfacial stability. *J. Power Sources* 329, 553–557. doi: 10.1016/j.jpowsour.2016.08.131

Wang, J., Li, X., Wang, Z., Guo, H., Li, Y., He, Z., et al. (2013a). Enhancement of electrochemical performance of Al-doped $LiVPO_4F$ using AlF_3 as aluminum source. *J. Alloys Comp.* 581, 836–842. doi: 10.1016/j.jallcom.2013.07.147

Wang, J., Li, X., Wang, Z., Huang, B., Wang, Z., and Guo, H. (2014). Nanosized $LiVPO_4F$/graphene composite: a promising anode material for lithium

ion batteries. *J. Power Sources* 251, 325–330. doi: 10.1016/j.jpowsour.2013.11.095

Wang, J., Wang, Z., Shen, L., Li, X., Guo, H., Tang, W., et al. (2013b). Synthesis and performance of $LiVPO_4F$/C-based cathode material for lithium ion battery. *T. Nonferr. Metal. Soc.* 23, 1718–1722. doi: 10.1016/S1003-6326(13)62653-9

Wu, L., Shi, S., Zhang, X., Yang, Y., Liu, J., Tang, S., et al. (2018). Room-temperature pre-reduction of spinning solution for the synthesis of $Na_3V_2(PO_4)_3$/C nanofibers as high-performance cathode materials for Na-ion batteries. *Electrochim. Acta* 274, 233–241. doi: 10.1016/j.electacta.2018.04.122

Wu, X., Li, Y., Liu, Z., Wu, X., Xiong, L., and Chen, J. (2016). The electrochemical performance of aqueous rechargeable battery of $Zn/Na_{0.44}MnO_2$ based on hybrid electrolyte. *J. Power Sources* 336, 35–39. doi: 10.1016/j.jpowsour.2016.10.053

Wu, X., Xiang, Y., Peng, Q., Wu, X., Li, Y., and Wu, X. M. (2017). A green-low-cost rechargeable aqueous zinc-ion battery using hollow porous spinel ZnMn2O4 as the cathode material. *J. Mater. Chem. A* 5,17990–17997. doi: 10.1039/c7ta00100b

Xiao, P., Lai, M., and Lu, L. (2013). Transport and electrochemical properties of high potential tavorite $LiVPO_4F$. *Solid State Ionics* 242, 10–19. doi: 10.1016/j.ssi.2013.04.002

Xu, G., Liu, Z., Zhang, C., Cui, G., and Chen, L. (2015). Strategies for improving the cyclability and thermo-stability of $LiMn_2O_4$-based batteries at elevated temperatures. *J. Mater. Chem. A* 3, 4092–4123. doi: 10.1039/c4ta06264g

Yamada, A., Hosoya, M., Chung, S., Kudo, Y., Hinokuma, K., Liu, K., et al. (2003). Olivine-type cathodes. *J. Power Sources* 119–121, 232–238. doi: 10.1016/S0378-7753(03)00239-8

Zhou, F., Zhao, X., and Dahn, J. R. (2009). Reactivity of charged $LiVPO_4F$ with 1M $LiPF_6$ EC: DEC electrolyte at high temperature as studied by accelerating rate calorimetry. *Electrochem. Commun.* 11, 589–591. doi: 10.1016/j.elecom.2008.12.052

Zhu, X., Liu, Y., Geng, L., and Chen, L. (2008). Synthesis and performance of lithium vanadium phosphate as cathode materials for lithium ion batteries by a sol-gel method. *J. Power Sources* 184, 578–582. doi: 10.1016/j.jpowsour.2008.01.007

Conflict of Interest Statement: The authors declare that the research was conducted in the absence of any commercial or financial relationships that could be construed as a potential conflict of interest.